

Shear Stress and Interlaminar Shear Strength Tests of Cross-laminated Timber Beams

Yao Lu, Wenbo Xie, Zheng Wang,* and Zizhen Gao

The interlaminar shear stresses of the three-layer, five-layer, and seven-layer cross laminated timber (CLT) and those of the oriented laminated beams were calculated according to Hooke's law and the differential relationship between the beam bending moment and shear force. The interlaminar and maximum shear stresses of the CLT beam are related to the number of CLT layers and to the elastic modulus ratio E_{\parallel}/E_{\perp} (or E_{\parallel}/E_R) of the parallel and perpendicular layers. The interlaminar shear strength of the Hemlock CLT was positively correlated with the elastic modulus of its parallel layer. The results showed that the CLT short-span beams had three failure modes when subjected to a three-point bending test, namely perpendicular layer rolling shear failure, CLT interlaminar shear failure, and parallel layer bending failure. The shear stress of the oriented laminated beam followed a parabolic distribution along the height of the section, while the shear stress of the orthogonally laminated beams tended to be balanced, rather than parabolically distributed along the height of section. The short beam three-point bending method was able to effectively test the interlaminar shear strength of CLT due to its stable and readable load.

Keywords: Cross-laminated timber; Interlaminar shear stress; Interlaminar shear strength; Test

Contact information: College of Materials Science and Engineering, Nanjing Forestry University, Nanjing, Jiangsu 210037, China; *Corresponding author: wangzheng63258@163.com

INTRODUCTION

Cross-laminated timber (CLT) is the basic unit of production for heavy wood structures used in mid- to high-rise buildings. The advantages of CLT as a building material include factory prefabrication, simple installation, light weight, high strength, good structural integrity, high thermal insulation performance, and durability (Que *et al.* 2017; Wang *et al.* 2017).

As a new solid wood composite building material, it is particularly important to control the design, processing technology, and processing parameters of CLT (Wang *et al.* 2011; Gagnon *et al.* 2012; Cao *et al.* 2016; Sikora *et al.* 2016). The interlaminar shear strength of CLT, which is widely used to evaluate the interlaminar mechanical properties of CLT, refers to the strength limit under shear stress between the laminates.

At present, the shear strength of CLT is commonly measured using the short beam bending method. In other words, to ensure shear failure rather than bending damage, CLT short beams are subjected to load measurement during the three-point bending test.

According to the ANSI/APA PRG 320-2012 standard (ANSI/APA PRG 320-2012), the span should be 5 to 6 times the thickness of the specimen when the interlaminar shear strength of the CLT is tested. The ASTM D198 standard (ASTM D-198-2015) shows that

the short beam three-point bending method is suitable for testing the interlaminar shear strength of engineered wood products with irregular sections, including those with rectangular sectional wood materials, wooden joists, and circular columns.

Moreover, the interlaminar shear strength of the rectangular section wood specimen is 1.5 times the average shear stress of the section, namely $3P/4bh$, where P is the interlaminar shear failure load of specimen, b is the width, and h is the thickness. It is uncertain whether the calculation formula of interlaminar shear strength based on the ASTM D198 standard is suitable for CLT. It is necessary to find a way to estimate the accuracy of the test. One of the purposes of this work is to solve these two problems.

In the current work, the formula describing the normal stress of the CLT beam along the height of the rectangular section was obtained first according to the orthogonal anisotropy of CLT. Then, the calculation formula for the shear stress of the CLT beam was derived according to the differential relationship between the bending moment and the shear on the beam section. After that, the interlaminar and maximum shear stresses of the three-layer, five-layer, and seven-layer CLT beams were calculated. The interlaminar shear strength of the CLT hemlock was measured using a short-span three-point bending method with a span-to-depth ratio of 6 (ANSI/APA PRG 320-2012, ASTM D-198-2015).

EXPERIMENTAL

Interlaminar Shear Strength Test of Three-layer CLT

According to the ANSI APA PRG320-2012 standard, the interlaminar shear strength of CLT was tested by means of short span three-point bending method.

The designed CLT boards had dimensions of 5,500 mm × 1,200 mm × 105 mm. Figure 1 shows the unit structure of the boards.

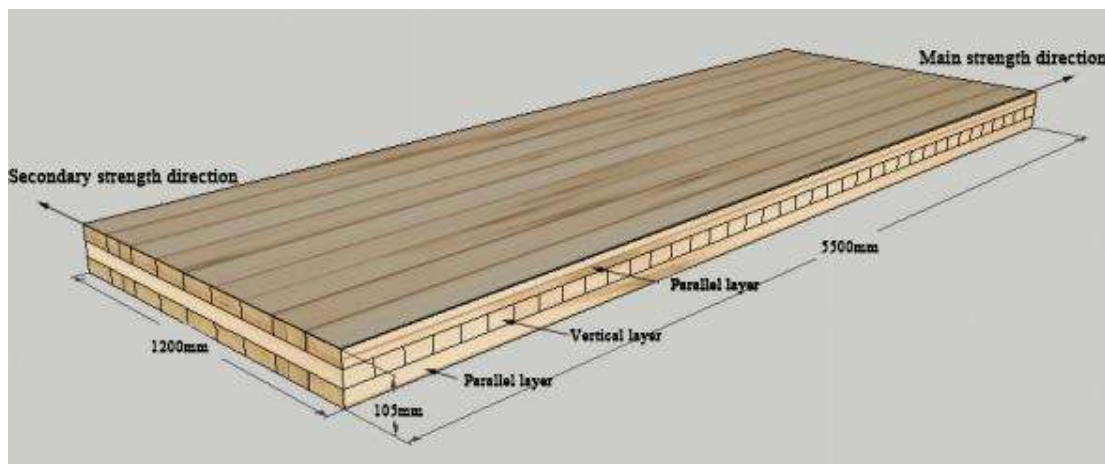


Fig. 1. CLT unit structure

The full-scale CLT boards (Fig. 1) were made on the CLT production line of the Ningbo Sino-Canada Low-Carbon Technology Research Institute Co., Ltd. according to the CLT manual (Wang *et al.* 2011) and conventional Canadian CLT production technology.

There are two types of full-scale CLT boards: those consisting of three parallel layers of Hemlock Grade 1 ($E=13.8$ GPa), and those consisting of three parallel layers of Hemlock Grade 2 ($E=10.3$ GPa). These layers were numbered 1, 2, 3, 4, 6, and 8. The perpendicular layers of the CLT boards of Grades 1 and 2 were comprised of the hemlock with an average elastic modulus of 7.4 GPa. From one full-size CLT board, four specimens ($735 \text{ mm} \times 305 \text{ mm} \times 105 \text{ mm}$) were obtained to achieve three-point bending with the span of 630 mm, *i.e.*, a span-to-depth ratio is 6.

The test instruments consisted of one universal mechanical testing machine with a maximum load of 10T (including one set of load displacement analysis software) produced by Jinan Tianchen Testing Machine Manufacturing Co., Ltd. and one self-made vacuum-pressurized circulation system, including a vacuum pressure tank (60 m^3), vacuum pump, air compressor, and tubes.

The interlaminar shear strength of the three-layer CLT was tested using the three-point bending method. The loading point was located in the middle of span, while the loading direction was perpendicular to the specimen surface (Fig. 2).

During the test, to record the load-displacement curve the loading rate was set as 4 mm/min. The failure location and failure mode of the specimen were represented by the point at which the load-displacement curve deviated from the characteristic of load-displacement curve. During the test, with the load-displacement curve was automatically recorded. The failure position, failure type, and the corresponding characteristics of load-displacement curve were observed until the specimen was destroyed. The load values were recorded when the interlaminar shear failure occurred in the specimens. It was found that interlaminar shear failure load was the maximum load in the load-displacement curve, from which the interlaminar shear strength of CLT could be calculated.

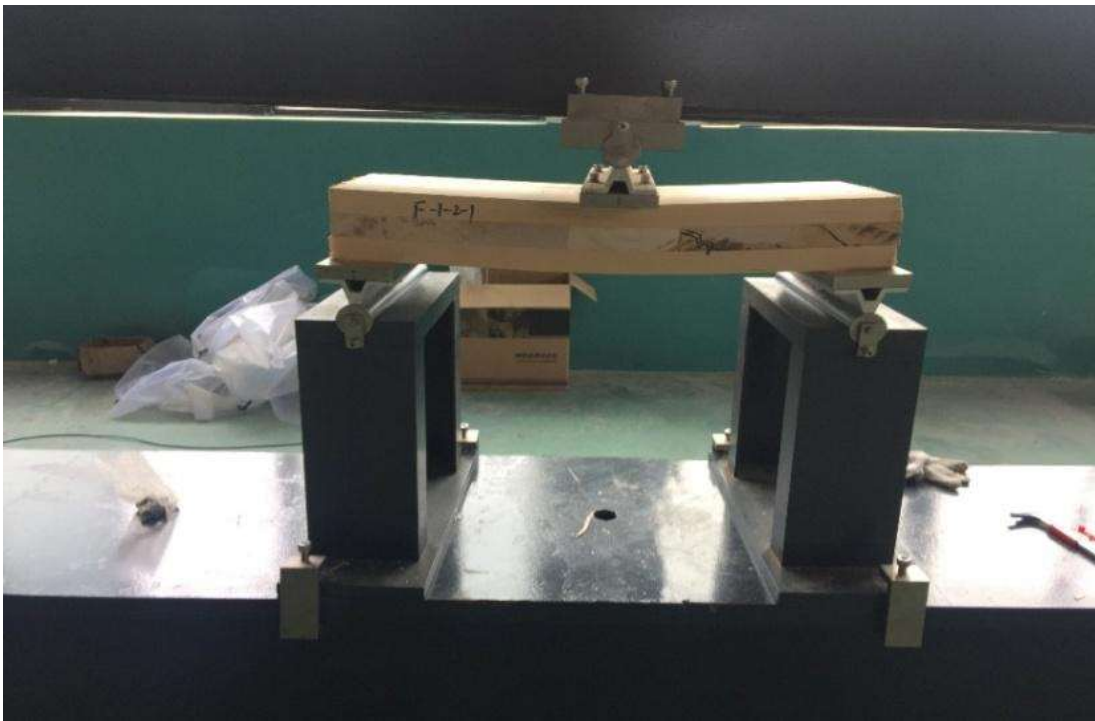


Fig. 2. Interlaminar shear strength test of CLT

Load-displacement Curve and Corresponding Failure Mode of CLT Three-Point Bending Test

In the three-point bending loading process, the load-displacement curve was recorded in order to be able to synchronously observe the failure mode of the specimen. When the first load peak appeared in load-displacement curve, the cross grain of the perpendicular layer of the specimen showed cracks and a sloping failure surface.

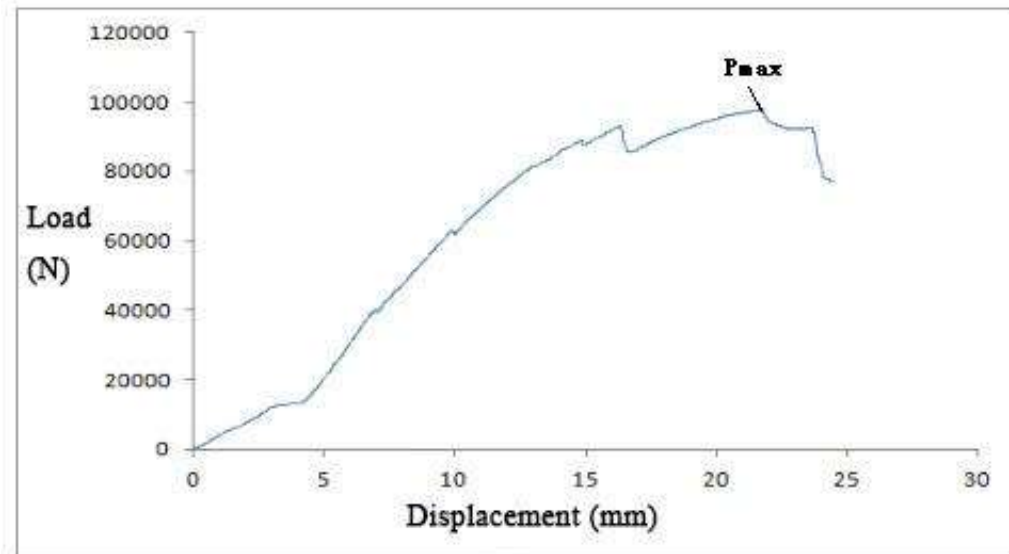


Fig. 3. Load-displacement curve of CLT three-point bending test



Fig. 4. Destruction surface of three-layer CLT short-span beam under three-point bending load

The failure mode during the loading process in the three-point bending test and the corresponding load in the load-displacement curve showed that the interlaminar shear failure load was the maximum load in the three-point bending load-displacement curve.

After local unloading, the displacement slowly increased with the reduction in the load. After that, the displacement could be increased only by increasing the load. The specimen suffered interlaminar shear failure when the second peak was reached, namely at the maximum load in the load-displacement curve. Then, the load decreased, first slowly, then sharply, with the increase in displacement. When the third peak occurred in the load-displacement curve, the parallel layer of the specimen was damaged by tensile fracture, resulting in the complete failure of the specimen (Figs. 3 and 4).

RESULTS AND DISCUSSION

Failure Mode of CLT Beam during Three-point Bending

When the span-to-depth ratio of the three-point bending specimen is less than 7, the effect of shear stress on beam deformation will rapidly increase with the decrease in span-to-depth ratio. For instance, when the span-to-depth ratios are 6, 5, and 4 for simple beams with concentrated force across the center, the percentages of bending deformation of the shear stress and bending moment were 7.9, 11.4, and 17.8%, respectively (Shao and Ma 1988). Therefore, the specimens with small span-to-depth ratios (6, 5, or 4) were applied to improve shear strength accuracy. In this work, the span-to-depth ratio of specimen in the test was 6.

When the CLT beam was loaded by short-span three-point bending, the failure location was close to the lower support. The failure surface was near the interface between the parallel and perpendicular layers, closer to the parallel layer. Wood chips could be found on the interlaminar shear failure surface, indicating that the failure was not due to insufficient cementing strength at the adhesive layer. The failure location near the lower support led to a small bending moment (namely normal stress) on the adjacent section. As there is a large shear stress at the interface between parallel and perpendicular layers, it is considered to be a virtually pure shear state. The interlayer bore most of the shear deformation, and the failure surface was the interlayer. Thus, the interlaminar shear strength of the CLT was the shear stress as determined by the interlaminar failure load.

Shear Stress Analysis of CLT beam

Normal stress of three-layer CLT beam

CLT beams with a parallel layer/perpendicular layer/parallel layer structure are orthotropic. The material property is symmetrical in the middle of the beam ($y = 0$, see Fig. 5(a)). When the beam bends, the longitudinal strain is represented by ε_x for the neutral axis $y = 0$. The longitudinal strain of the beam changes linearly with y ($\varepsilon_x = \kappa y$), where κ is the curvature of beam. In other words, ε_x had linear variation along the section depth.

The strain at the junction of the parallel and perpendicular layers was continuous (Timoshenko and Gere 1978). The parallel and perpendicular layers had different elastic moduli E_1 and E_2 (Wang *et al.* 2016). Therefore, the normal stress of the CLT beams was discontinuous at the junction of the parallel and perpendicular layers, and there was a hop (Fig. 5 (b)).

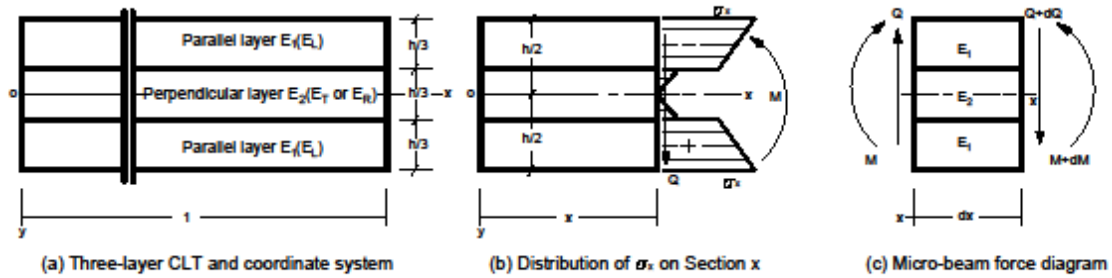


Fig. 5. Three -layer CLT coordinate system and normal stress distribution

According to Hooke's law, the normal stress σ_x of the CLT beam on Section x could be expressed as,

$$\begin{aligned} \sigma_x &= E_1 \varepsilon = E_1 \kappa y, h/6 \leq |y| \leq h/2 \\ \sigma_x &= E_2 \varepsilon = E_2 \kappa y, 0 \leq |y| \leq h/6 \end{aligned} \tag{1}$$

where κ is the neutral layer curvature of beam, E_1 is the elastic modulus of the parallel layer; E_2 represents the elastic modulus of the perpendicular layer, and h is the height of the rectangular section of beam.

The composite bending moment of σ_x on Section x could be expressed as

$$M = \int_A \sigma_x y dA$$

Formula (1) was substituted to derive

$$M = 2 \left[\int_{h/6}^{h/2} E_1 \kappa y^2 b dy + \int_0^{h/6} E_2 \kappa y^2 b dy \right]$$

$$M = \kappa E_1 I \left(\frac{26}{27} + \frac{E_2}{27 E_1} \right),$$

$$\kappa = \frac{M}{E_1 I \left(\frac{26}{27} + \frac{E_2}{27 E_1} \right)}$$

where $I = \frac{1}{12} b h^3$, and b is the width of rectangular section of beam.

Then, the normal stresses of the three-layer CLT beam on Section x could be expressed as

$$\begin{aligned} \sigma_x &= E_1 \varepsilon = E_1 \kappa y = \frac{My}{I \left(\frac{26}{27} + \frac{E_2}{27 E_1} \right)}, h/6 \leq |y| \leq h/2 \\ \sigma_x &= E_2 \varepsilon = E_2 \kappa y = \frac{My}{I \left(\frac{26}{27} + \frac{E_2}{27 E_1} \right)} \frac{E_2}{E_1}, 0 \leq |y| \leq h/6 \end{aligned} \tag{2}$$

Shear stress of three-layer CLT beam

On the transverse section of the bending beam, the bending moment M and shear stress Q satisfied the following differential relationship (see Fig. 5 (c)),

$$\frac{dM}{dx} = Q \tag{3}$$

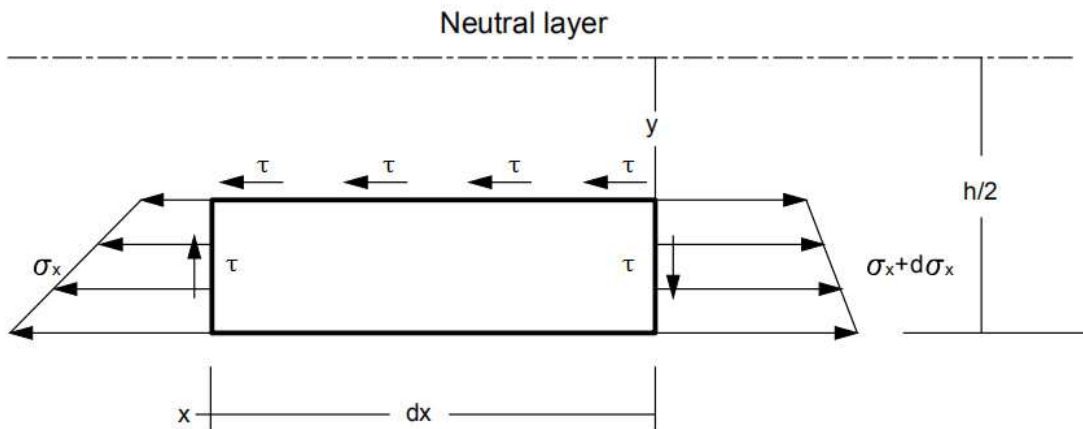


Fig. 6. Force diagram of an element in the CLT beam

When $h/6 \leq |y| \leq h/2$, given the equilibrium condition of the micro-segment separators (x and $x + dx$) in the x -direction Fig. 6), the following was true:

$$\begin{aligned} \tau b dx &= \int_y^{h/2} (\sigma_x + d\sigma_x) b dy - \int_y^{h/2} \sigma_x b dy = \int_y^{h/2} d\sigma_x b dy \\ \tau &= \int_y^{h/2} \frac{d\sigma_x}{dx} dy \end{aligned}$$

According to Formula (A-2,A-3),

$$\begin{aligned} \tau &= \int_y^{h/2} \frac{dM}{dx} \frac{y}{I(\frac{26}{27} + \frac{E_2}{27E_1})} dy = \frac{Q}{2I(\frac{26}{27} + \frac{E_2}{27E_1})} (\frac{h^2}{4} - y^2) \\ \tau &= \frac{3Q}{2A(\frac{26}{27} + \frac{E_2}{27E_1})} (1 - 4y^2 / h^2) \end{aligned} \tag{4}$$

From Formula (4), when $y = h/6$, the shear stress could be expressed as

$$\begin{aligned} \tau &= 0.8889 \frac{3Q}{2A} (E_1 / E_2 = 1) \\ \tau &= 0.9195 \frac{3Q}{2A} (E_1 / E_2 = 10) \end{aligned}$$

$$\tau = 0.9213 \frac{3Q}{2A} (E_1 / E_2 = 20)$$

$$\tau = 0.9219 \frac{3Q}{2A} (E_1 / E_2 = 30)$$

The CLT beam experienced continuous shear stress at the junction of its parallel and perpendicular layers. However, the normal stress in the section was discontinuous at the junction of the parallel and perpendicular layers (with a jump).

When $0 \leq |y| \leq h/6$,

$$\begin{aligned} \tau &= \frac{Q}{I} \int_{h/6}^{h/2} \frac{y}{\left(\frac{26}{27} + \frac{E_2}{27E_1}\right)} dy + \frac{Q}{I} \int_y^{h/6} \frac{y}{\left(\frac{26}{27} + \frac{E_2}{27E_1}\right)} \frac{E_2}{E_1} dy \\ \tau &= \frac{3Q}{2A \left(\frac{26}{27} + \frac{E_2}{27E_1}\right)} \left[\frac{8}{9} + \frac{E_2}{9E_1} (1 - 36y^2 / h^2) \right] \end{aligned} \quad (5)$$

From Formula (A-5), when $y = 0$, the shear stress could be expressed as

$$\tau = \frac{3Q}{2A} (E_1 / E_2 = 1), \tau = 0.9310 \frac{3Q}{2A} (E_1 / E_2 = 10)$$

$$\tau = 0.9271 \frac{3Q}{2A} (E_1 / E_2 = 20), \tau = 0.9257 \frac{3Q}{2A} (E_1 / E_2 = 30)$$

Stress of Five-layer CLT Beam

Normal stress of five-layer CLT beam

The five-layer CLT had a normal stress calculation similar to that of the three-layer laminated wood beam. First, the normal stresses of the parallel and the perpendicular layers were expressed as the elastic moduli and beam bending curvatures. After that, the normal stresses synthesized the bending moment of the section to derive the normal stress of the five-layer CLT as follows:

$$\begin{aligned} \sigma_x &= \frac{My}{I \left(\frac{99}{125} + \frac{26E_2}{125E_1} \right)}, 3h/10 \leq |y| \leq h/2 \\ \sigma_x &= \frac{My}{I \left(\frac{99}{125} + \frac{26E_2}{125E_1} \right)} \frac{E_2}{E_1}, h/10 \leq |y| \leq 3h/10 \\ \sigma_x &= \frac{My}{I \left(\frac{99}{125} + \frac{26E_2}{125E_1} \right)}, 0 \leq |y| \leq h/10 \end{aligned} \quad (6)$$

Shear stress of five-layer CLT beam

When $3h/10 \leq |y| \leq h/2$,

$$\tau = \int_y^{h/2} \frac{dM}{dx} \frac{y}{I \left(\frac{99}{125} + \frac{26E_2}{125E_1} \right)} b dy = \frac{Qb}{2I \left(\frac{99}{125} + \frac{26E_2}{125E_1} \right)} \left(\frac{h^2}{4} - y^2 \right) \quad (7)$$

From Formula (8), when $y = 3h/10$, the shear stress was

$$\tau = \frac{3Q}{2A \left(\frac{99}{125} + \frac{26E_2}{125E_1} \right)} \frac{16}{25}$$

$$\tau = 0.6400 \frac{3Q}{2A} (E_1/E_2 = 1)$$

$$, \tau = 0.7874 \frac{3Q}{2A} (E_1/E_2 = 10)$$

$$\tau = 0.7976 \frac{3Q}{2A} (E_1/E_2 = 20)$$

$$\tau = 0.8011 \frac{3Q}{2A} (E_1/E_2 = 30)$$

When $h/10 \leq |y| \leq 3h/10$,

$$\tau = \frac{Q}{I} \int_{3h/10}^{h/2} \frac{y}{\left(\frac{99}{125} + \frac{26E_2}{125E_1} \right)} b dy + \frac{Q}{I} \int_y^{3h/10} \frac{y}{\left(\frac{99}{125} + \frac{26E_2}{125E_1} \right)} \frac{E_2}{E_1} b dy \quad (8)$$

$$\tau = \frac{3Q}{2A \left(\frac{99}{125} + \frac{26E_2}{125E_1} \right)} \frac{16}{25} + \frac{3Q}{2A} \frac{1}{\left(\frac{99}{125} + \frac{26E_2}{125E_1} \right)} \frac{E_2}{E_1} 4(9/100 - y^2/h^2)$$

From Formula (8), when $y = h/10$, the shear stress was

$$\tau = \frac{3Q}{2A \left(\frac{99}{125} + \frac{26E_2}{125E_1} \right)} \frac{16}{25} + \frac{3Q}{2A} \frac{1}{\left(\frac{99}{125} + \frac{26E_2}{125E_1} \right)} \frac{E_2}{E_1} \frac{8}{25}$$

$$\tau = 0.96 \frac{3Q}{2A} (E_1/E_2 = 1)$$

$$\tau = 0.8268 \frac{3Q}{2A} (E_1/E_2 = 10)$$

$$\tau = 0.8175 \frac{3Q}{2A} (E_1/E_2 = 20)$$

$$\tau = 0.8145 \frac{3Q}{2A} (E_1/E_2 = 30)$$

When $0 \leq |y| \leq h/10$,

$$\tau = \frac{Q}{I} \left[\int_{3h/10}^{h/2} \frac{y}{\left(\frac{99}{125} + \frac{26E_2}{125E_1}\right)} bdy + \int_{h/10}^{3h/10} \frac{y}{\left(\frac{99}{125} + \frac{26E_2}{125E_1}\right)} \frac{E_2}{E_1} bdy + \int_y^{h/10} \frac{y}{\left(\frac{99}{125} + \frac{26E_2}{125E_1}\right)} \frac{E_2}{E_1} bdy \right]$$

$$\tau = \frac{3Q}{2A} \left[\frac{16}{25\left(\frac{99}{125} + \frac{26E_2}{125E_1}\right)} + \frac{8}{25\left(\frac{99}{125} + \frac{26E_2}{125E_1}\right)} \frac{E_2}{E_1} + \frac{1}{25\left(\frac{99}{125} + \frac{26E_2}{125E_1}\right)} (1 - 100y^2/h^2) \right] \quad (9)$$

From Formula (9), when $y = 0$, the shear stress was

$$\tau = \frac{3Q}{2A} (E_1/E_2 = 1)$$

$$\tau = 0.8760 \frac{3Q}{2A} (E_1/E_2 = 10)$$

$$\tau = 0.8674 \frac{3Q}{2A} (E_1/E_2 = 20)$$

$$\tau = 0.8645 \frac{3Q}{2A} (E_1/E_2 = 30)$$

Stress of Seven-layer CLT Beam

Normal stress of seven-layer CLT beam

The seven-layer CLT had normal stress calculations similar to those of the three-layer laminated wood beam. First, the normal stresses of the parallel and perpendicular layers were expressed as elastic moduli and beam bending curvatures. After that, the normal stresses synthesized the bending moment to obtain the normal stress of the seven-layer CLT.

$$\sigma_x = \frac{My}{I\left(\frac{244}{343} + \frac{99E_2}{343E_1}\right)}, 5h/14 \leq |y| \leq h/2$$

$$\sigma_x = \frac{My}{I\left(\frac{244}{343} + \frac{99E_2}{343E_1}\right)} \frac{E_2}{E_1}, 3h/14 \leq |y| \leq 5h/14$$

$$\sigma_x = \frac{My}{I\left(\frac{244}{343} + \frac{99E_2}{343E_1}\right)}, h/14 \leq |y| \leq 3h/14$$

$$\sigma_x = \frac{My}{I\left(\frac{244}{343} + \frac{99E_2}{343E_1}\right)} \frac{E_2}{E_1}, 0 \leq |y| \leq h/10 \quad (10)$$

Shear stress of seven-layer CLT beam

The interlayer shear stress calculation process for the three-layer and five-layer CLT showed that the following four integrals needed to be calculated to obtain the interlaminar shear stress of seven-layer CLT.

When $5h/14 \leq |y| \leq h/2$:

$$\tau = \frac{Q}{I} \int_y^{h/2} \frac{y}{\left(\frac{244}{343} + \frac{99E_2}{343E_1}\right)} bdy = \frac{3Q}{2A} \frac{1}{\left(\frac{244}{343} + \frac{99E_2}{343E_1}\right)} (1 - 4y^2/h^2) \quad (11)$$

When $3h/14 \leq |y| \leq 5h/14$:

$$\tau = \frac{Q}{I} \int_y^{5h/14} \frac{y}{\left(\frac{244}{343} + \frac{99E_2}{343E_1}\right)} \frac{E_2}{E_1} bdy = \frac{3Q}{2A} \frac{1}{\left(\frac{244}{343} + \frac{99E_2}{343E_1}\right)} \frac{E_2}{E_1} 4(25/196 - y^2/h^2) \quad (12)$$

When $h/14 \leq |y| \leq 3h/14$:

$$\tau = \frac{Q}{I} \int_y^{3h/14} \frac{y}{\left(\frac{244}{343} + \frac{99E_2}{343E_1}\right)} bdy = \frac{3Q}{2A} \frac{1}{\left(\frac{244}{343} + \frac{99E_2}{343E_1}\right)} 4(9/196 - y^2/h^2) \quad (13)$$

When $0 \leq |y| \leq h/14$:

$$\tau = \frac{Q}{I} \int_y^{h/14} \frac{y}{\left(\frac{244}{343} + \frac{99E_2}{343E_1}\right)} \frac{E_2}{E_1} bdy = \frac{3Q}{2A} \frac{1}{\left(\frac{244}{343} + \frac{99E_2}{343E_1}\right)} \frac{E_2}{E_1} 4(1/196 - y^2/h^2) \quad (14)$$

If $y = 5h/14$, then the shear stress could be expressed as

$$\tau = 0.4898 \frac{3Q}{2A} (E_1/E_2 = 1)$$

$$\tau = 0.6617 \frac{3Q}{2A} (E_1/E_2 = 10)$$

$$\tau = 0.6748 \frac{3Q}{2A} (E_1/E_2 = 20)$$

$$\tau = 0.6793 \frac{3Q}{2A} (E_1/E_2 = 30)$$

If $y = 3h/14$, then the shear stress was

$$\tau = 0.8164 \frac{3Q}{2A} (E_1/E_2 = 1)$$

$$\tau = 0.7059 \frac{3Q}{2A} (E_1/E_2 = 10)$$

$$\tau = 0.6972 \frac{3Q}{2A} (E_1/E_2 = 20)$$

$$\tau = 0.6943 \frac{3Q}{2A} (E_1/E_2 = 30)$$

If $y = h/14$, then the shear stress was

$$\tau = 0.9797 \frac{3Q}{2A} (E_1/E_2 = 1)$$

$$\tau = 0.9265 \frac{3Q}{2A} (E_1/E_2 = 10)$$

$$\tau = 0.9221 \frac{3Q}{2A} (E_1/E_2 = 20)$$

$$\tau = 0.9207 \frac{3Q}{2A} (E_1/E_2 = 30)$$

If $y = 0$, then the shear stress was

$$\tau = 0.4898 \frac{3Q}{2A} (E_1/E_2 = 1)$$

$$\tau = 0.9288 \frac{3Q}{2A} (E_1/E_2 = 10)$$

$$\tau = 0.9235 \frac{3Q}{2A} (E_1/E_2 = 20)$$

$$\tau = 0.9216 \frac{3Q}{2A} (E_1/E_2 = 30)$$

Based on the shear stress analysis and results of CLT beam, the ratios of the interlaminar shear stresses (three-layered, five-layered, and the seven-layered CLT) and the maximum shear stress of the equidirectional laminated wood ($1.5Q/A$) were obtained (Table 1).

Table 1. Interlaminar Shear Stress ($\tau/1.5\tau_{av}$) of CLT, $\tau_{av} = Q/A$, $A = bh$

CLT	Y-coordinate	E_1/E_2			
		1	10	20	30
Three layers	$h/2$	0	0	0	0
	$h/6$	0.8889	0.9195	0.9213	0.9219
	0	1	0.9310	0.9271	0.9257
Five layers	$h/2$	0	0	0	0
	$3h/10$	0.6400	0.7874	0.7976	0.8011
	$h/10$	0.9600	0.8268	0.8175	0.8145
	0	1	0.8760	0.8674	0.8645
Seven layers	$h/2$	0	0	0	0
	$5h/14$	0.4898	0.6617	0.6748	0.6793
	$3h/14$	0.8164	0.7059	0.6972	0.6943
	$h/14$	0.9796	0.9495	0.9273	0.9243
	0	1	0.9524	0.9288	0.9252

Figures 7 and 8 show the distributions of interlaminar shear stress of the five-layer and seven-layer CLT beams ($E_1/E_2 = 20$), respectively, compared to the equidirectional laminated timber beams ($E_1/E_2 = 1$).

For the five-layer, seven-layer, and equidirectional laminated timber beams ($E_1/E_2 = 1$), the shear stress followed approximately a parabolic distribution along the depth of section. This was consistent with the fact that the shear stress of the isotropic material beam followed a parabolic distribution along the depth of the section height.

The shear stress of the orthogonal laminated timber beam did not continue to follow the parabolic distribution along the depth of the section, but showed a balanced value along the height variation. The maximums, located in the neutral layer, were about 87 and 93% of 1.5 times that of the average shear stress, respectively.

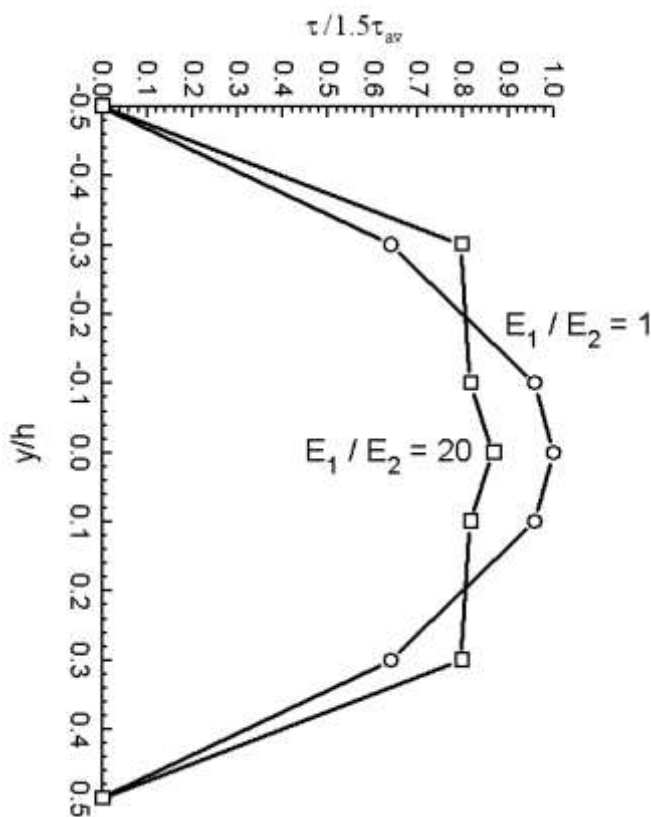


Fig. 7. Distributions of interlaminar shear stress of five-layer CLT beam ($E_1/E_2 = 20$) and equidirectional laminated timber beam ($E_1/E_2 = 1$) along height of the section

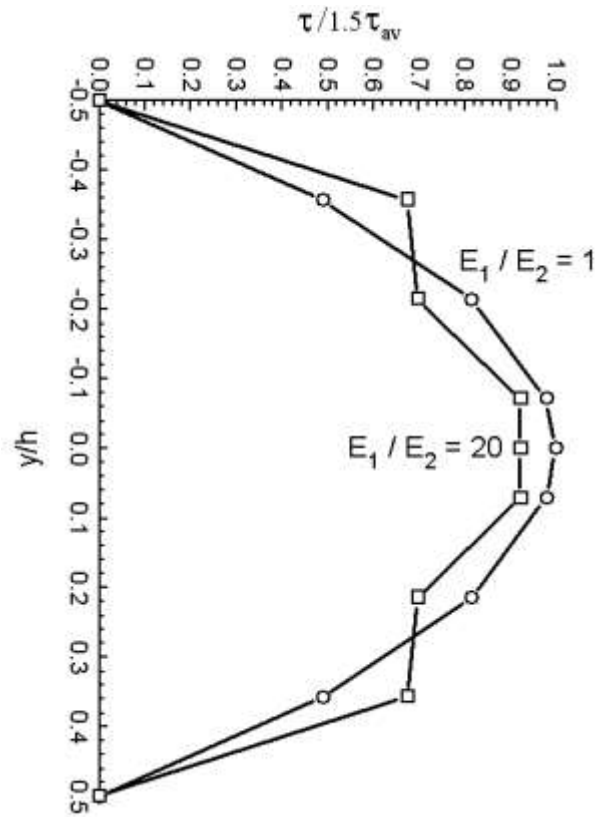


Fig. 8. Distributions of interlaminar shear stress of seven-layer CLT beam ($E_1/E_2 = 20$) and equidirectional laminated timber beam ($E_1/E_2 = 1$) along the height of section

Interlaminar Shear Strength of CLT

According to the data in Table 1, the maximum interlaminar shear stress of CLT beam was expressed as

$$\tau = k_{eff} \frac{3Q}{2A} \quad (15)$$

where K_{eff} is defined as the ratio between the maximum interlaminar shear stress and 1.5 times of the average shear stress on the cross section of CLT beam, K_{eff} is related to E_1/E_2 , the number of orthogonal laminated layers and the locations of the layers in the section,

The elastic modulus ratio E_1/E_2 of CLT was usually larger than 10. Therefore, the correction coefficient K_{eff} in the formula depended mainly on the number of layers of CLT (Table 1).

When the three-layer CLT was loaded in the three-point bending test, the interlaminar shear failure surface was close to the lower support and near the interface between the parallel and perpendicular layers. Here, the bending moment was small, and the shear stress was $Q = P/2$. Therefore, the normal bending stress, which was small relative to the shear stress, could be ignored. The interlaminar damage surface was near the interface between the parallel and perpendicular layers, inclining to the parallel layer.

Given $y=h/6$, the correction coefficient $K_{eff} \approx 0.92$. In the three-point bending test, the interlaminar shear strength of the three-layer CLT could be expressed as

$$\tau = 0.92 \frac{3P_{\max}}{4bh} \quad (16)$$

where τ is the interlaminar shear strength of CLT (MPa), P_{\max} is the maximum load in the load-displacement curve (N), b is the width of specimen (mm), and h is the thickness of specimen (mm).

According to Table 1, for the five-layer CLT, $K_{eff} \approx 0.82$, while for seven-layer CLT, $K_{eff} \approx 0.93$. Therefore, the interlaminar shear strength of the five-layer CLT could be expressed as $\tau = 0.82 \frac{3P_{\max}}{4bh}$, while the interlaminar shear strength of the seven-layer CLT

could be expressed as $\tau = 0.93 \frac{3P_{\max}}{4bh}$.

Table 2. Interlaminar Shear Strength Test Results of Three-layer CLT Hemlock with Grade 1 along the Main Strength Direction

Specimen No.	P_{\max} (kN)	Interlaminar Shear Strength (MPa)	Average Interlaminar Shear Strength (MPa)
1-1	106.40	2.29	2.16
1-2	96.57	2.06	
1-3	96.47	2.12	
1-4	97.75	2.18	
2-1	86.68	1.89	1.97
2-2	97.84	2.11	
2-3	82.00	1.76	
2-4	97.12	2.12	
3-1	95.11	2.08	2.04
3-2	82.00	1.78	
3-3	103.50	2.34	
3-4	86.00	1.94	
Average (Coefficient of Variation)		2.06 (8.8%)	

Tables 2 and 3 show the interlaminar shear strengths of the three-layer CLT hemlock with Grades 1 and 2 along the main strength direction as determined by the test.

Table 3. Interlaminar Shear Strength Test Results of Three-layer CLT Hemlock with Grade 2 along the Main Strength Direction

Specimen No.	P_{max} (kN)	Interlaminar Shear Strength (MPa)	Average Interlaminar Shear Strength (MPa)
4-1	76.81	1.67	1.58
4-2	69.07	1.53	
4-3	62.66	1.37	
4-4	78.32	1.73	
6-1	82.86	1.82	1.71
6-2	77.60	1.68	
6-3	80.66	1.77	
6-4	71.76	1.57	
8-1	85.04	1.81	1.90
8-2	100.60	2.13	
8-3	83.71	1.81	
8-4	85.16	1.85	
Average (Coefficient of Variation)		1.73 (11.0%)	

The hemlocks are classified according to E_L values. For hemlock CLT of Grades 1 and 2, the interlaminar shear strengths were 2.06 and 1.73 MPa, respectively, with a difference of 19%. Therefore, the interlaminar shear strength of CLT was positively correlated with the elastic modulus of the CLT parallel layer. This explains the importance of wood classification in engineering applications.

CONCLUSIONS

1. For the beams with equidirectional laminated timber, the shear stress followed approximately a parabolic distribution along the height of rectangular section. The shear stresses on the upper and lower edge points of the section were equal to zero. On the neutral layer, the shear stress reached the maximum, namely 1.5 times that of the average shear stress of the section.
2. The shear stress of CLT beam no longer approximately follows a parabolic distribution along the height of rectangular section. With the increase of CLT layers, the shear stress on the cross section tends to be more uniformly distributed. The maximum shear stress is less than 1.5 times of the average shear stress on the cross section. Its value is related to number of layers, parallel layer, perpendicular layer and the ratio between elastic modulus of parallel and perpendicular layer E_1/E_2 .
3. During the three-point bending test, the CLT short span beam exhibited three failure modes, namely perpendicular layer rolling shear, CLT interlaminar, and parallel layer bending failures.

4. For the three-point bending tests of three-layer, five-layer, and seven-layer CLT short span beams, the interlaminar shear strengths could be uniformly expressed as $\tau = k_{\text{eff}} \frac{3P_{\text{max}}}{4bh}$, where K_{eff} values were 0.92, 0.82, and 0.93, respectively, and P_{max} was determined by the maximum load of the load-displacement curve recorded in the three-point bending tests.
5. The interlaminar shear strength of CLT was positively correlated with the elastic modulus of the parallel layer. Grading the timbers according to the elastic modulus could improve the interlaminar shear strength of CLT.

ACKNOWLEDGEMENTS

This study was funded by the Priority Academic Program Development of Jiangsu Higher Education Institutions (PAPD) and the 2017 Jiangsu Province Forestry Science and Technology Innovation and Extension Fund (LYKJ[2017]41).

REFERENCES CITED

- ANSI/APA PRG 320-2012. "Standard for performance-rated cross-laminated timber," New York, USA.
- ASTM D-198-2015. "Standard test methods of static tests of lumber in structural sizes," Pennsylvania, USA.
- Cao, Y., Wang, Y. L., and Wang, Z. (2016). "Application and research progress of overseas cross-laminated timber (CLT) construction," *China Forest Products Industry* 13(12), 3-7. DOI: 10.3969/j.issn.1001-5299.2016.12.001
- Gagnon, S., Bilek, E. M., Podsto, L. Crespell, P., Gagnon, S., and Bilek, E. M. (2012). *CLT Handbook: Cross-laminated Timber*, FPInnovation, New York, USA.
- Que, Z. L., Li, Z. R., and Wang, F. B. (2017). "Review of research and development status of cross-laminated timber used by medium high-rise structure in Europe," *Building Structure* 47(2), 75-80+27. DOI:1002-848X(2017) 02-0075-06
- Shao, B., and Ma, G. X. (1988). "Analysis of effect of shear on deformation of beams," *Journal of Nanjing Institute of Chemical Technology* 10(3), 78-84. DOI: 1671-7627/CN:32-1670/N.
- Sikora, K. S., McPolin, D. O., and Harte, A. M. (2016). "Effects of the thickness of cross-laminated timber (CLT) panels made from Irish Sitka spruce on mechanical performance in bending and shear," *Construction and Building Materials* 116(7), 141-150. DOI: 10.1016/j.conbuildmat.2016.04.145.
- Timoshenko, S., and Gere, J. (1978). *Mechanics of Material*, Science Press, Beijing, China
- Wang, B. J., Pirvu, C., and Lum, C. (2011). "Cross-laminated timber manufacturing," in: *Canadian CLT Handbook*, FPInnovations, Quebec, Canada
- Wang, Z., Gao, Z. Z., and Cao, Y. (2016). "Dynamic measuring Poisson's Ratio μ_{LT} , μ_{LR} and μ_{RT} of lumbers by electrical method," *Scientia Silvae Sinicae* 52(8), 104-114. DOI:10.11707/j.1001-7488.20160813.

Wang, Y. L., Wang, Z., and Wang, J. H. (2017). “Research progress of the new generation of heavy CLT wood structure building technology,” *Journal of Northwest Forestry University* 32(2), 286-293. DOI: 10.3969/j.issn.1001-7461.2017.02.50.

Article submitted: January 19, 2018; Peer review completed: March 17, 2018; Revised version received and accepted: May 18, 2018; Published: May 23, 2018.
DOI: 10.15376/biores.13.3.5343-5359